ELSEVIER

Mechanisms of Development 121 (2004) 673–685

www.elsevier.com/locate/modo

Research paper

Genetic dissection of the formation of the forebrain in Medaka, *Oryzias latipes*

Daiju Kitagawa[a], Tomomi Watanabe[a], Kota Saito[a], Satoshi Asaka[a], Takao Sasado[b], Chikako Morinaga[b], Hiroshi Suwa[b], Katsutoshi Niwa[b], Akihito Yasuoka[c], Tomonori Deguchi[d], Hiroki Yoda[d], Yukihiro Hirose[e], Thorsten Henrich[b], Norimasa Iwanami[f], Sanae Kunimatsu[f], Masakazu Osakada[g], Chritoph Winkler[h], Harun Elmasri[h], Joachim Wittbrodt[i], Felix Loosli[i], Rebecca Quiring[i], Matthias Carl[i], Clemens Grabher[i], Sylke Winkler[i], Filippo Del Bene[i], Akihiro Momoi[d], Toshiaki Katada[a], Hiroshi Nishina[a], Hisato Kondoh[b,d], Makoto Furutani-Seiki[b,*]

[a]*Department of Physiological Chemistry, Graduate School of Pharmaceutical Sciences, The University of Tokyo, Tokyo 113-0033, Japan*
[b]*Japan Science and Technology Agency, ERATO, Kondoh Differentiation Signaling Project, Kawaracho14, Yoshida, Sakyoku, Kyoto 606-8305, Japan*
[c]*Graduate School of Agricultural and Life Sciences, The University of Tokyo, Tokyo 113-0033, Japan*
[d]*Graduate School of Frontier Biosciences, Osaka University, Osaka, 565-0871, Japan*
[e]*Graduate School of Biostudies, Kyoto University, Kyoto 606-8502, Japan*
[f]*Division of Experimental Immunology, Institute for Genome Research, The University of Tokushima, Tokushima 770-8503, Japan*
[g]*Department of Molecular Medicine and Pathophysiology, Research Institute, Osaka Medical Center for Cancer and Cardiovascular Diseases, Osaka 537-8511, Japan*
[h]*Department of Physiological Chemistry I, Biocenter, University of Wuerzburg, Wuerzburg, Germany*
[i]*Developmental Biology Programme, EMBL, D-69117, Heidelberg, Germany*

Received 1 February 2004; received in revised form 16 March 2004; accepted 18 March 2004

Abstract

The forebrain, consisting of the telencephalon and diencephalon, is essential for processing sensory information. To genetically dissect formation of the forebrain in vertebrates, we carried out a systematic screen for mutations affecting morphogenesis of the forebrain in Medaka. Thirty-three mutations defining 25 genes affecting the morphological development of the forebrain were grouped into two classes. Class 1 mutants commonly showing a decrease in forebrain size, were further divided into subclasses 1A to 1D. Class 1A mutation (1 gene) caused an early defect evidenced by the lack of *bf1* expression, Class 1B mutations (6 genes) patterning defects revealed by the aberrant expression of regional marker genes, Class 1C mutation (1 gene) a defect in a later stage, and Class 1D (3 genes) a midline defect analogous to the zebrafish *one-eyed pinhead* mutation. Class 2 mutations caused morphological abnormalities in the forebrain without considerably affecting its size, Class 2A mutations (6 genes) caused abnormalities in the development of the ventricle, Class 2B mutations (2 genes) severely affected the anterior commissure, and Class 2C (6 genes) mutations resulted in a unique forebrain morphology. Many of these mutants showed the compromised *sonic hedgehog* expression in the zona-limitans-intrathalamica (zli), arguing for the importance of this structure as a secondary signaling center. These mutants should provide important clues to the elucidation of the molecular mechanisms underlying forebrain development, and shed new light on phylogenically conserved and divergent functions in the developmental process.

Keywords: Forebrain; Telencephalon; Diencephalon; Mutants; Medaka; Mutagenesis screen

1. Introduction

The vertebrate forebrain, consisting of the telencephalon and diencephalon, is formed at the most rostral portion of the developing central nervous system (CNS). The telencephalon is the highest-order processor of neural functions,

* Corresponding author. Tel./fax: +81-75-771-9362.
E-mail address: furutaniseiki@msi.biglobe.ne.jp (M. Furutani-Seiki).

0925-4773/$ - see front matter © 2004 Elsevier Ireland Ltd. All rights reserved.
doi:10.1016/j.mod.2004.03.010

and the diencephalon is the conduit for ascending sensory information. Each territory of the forebrain is further regionalized along the respective anteroposterior (AP) and dorsoventral (DV) axes. These structures in the forebrain and their connections are essential for processing sensory information, integrating of new sensory information with established memories, and then formulating and effecting behavioral responses (Wilson and Rubenstein, 2000; Rallu et al., 2002).

The vertebrate forebrain was proposed to be subdivided in a segment-like manner into transverse neuromeric domains (prosomeres) analogous to rhombomeres in the hindbrain; on the basis of restricted expression patterns of transcription factors (neuromeric model, Bulfone et al., 1993; Figdor and Stern, 1993; Puelles and Rubenstein, 1993; Hauptmann and Gerster, 2000).

In all vertebrates, the developing telencephalon is subdivided into the dorsal (pallial region, expressing *emx1*) and ventral (subpallial region, expressing *dlx2*) domains. In the mammalian telencephalon, dorsal, pallial regions give rise to the cortex, while ventral, subpallial regions give rise to the basal ganglia. Similar pallial and subpallial subdivisions of the telencephalon exist in all vertebrates (Fernandez et al., 1998; Puelles et al., 2000), although the adult derivatives of these subdivisions vary among species.

The diencephalon is proposed to be divided into four longitudinal neuronal zones—dorsally, epithalamus, dorsal thalamus, ventral thalamus; and ventrally, hypothalamus (Figdor and Stern, 1993; Hauptmann et al., 2002). The dorsal and ventral thalami are divided by the zona limitans intrathalamica (zli). Although it is yet to be proven, the zli has been suggested to be a secondary signaling center, since the secreted signaling protein *sonic hedgehog* (*shh*) is expressed in the zli.

Theories of the formation of the subdivisions of the forebrain, however, are established on the bases of restricted expression patterns, mostly of transcription factors. Most of these transcription factors were cloned either by the homology of genes identified in the forward genetic mutant screening of invertebrates, such as *Drosophila melanogaster* and *Caenorhabditis elegans*, or by expression pattern screening. Functional studies of these genes have been carried out by the reverse genetic approach in the mouse or gain-of-function studies in chick, *Xenopus* and zebrafish. These studies, however, were still limited to the genes initially cloned by homology or expression patterns, but not their functions.

Genome-wide forward genetic screening based on the functions of genes, carried out using zebrafish for the first time in vertebrates, together with gene knock-out mice, established a genetic basis for the three key signaling pathways for the patterning of the forebrain. The Nodal pathway acts upstream of Shh signaling to specify the ventral telencephalon (Rohr et al., 2001; Varga et al., 2001), but Nodal and Shh signaling have distinct and cooperative roles in the development of the ventral diencephalon (Mathieu et al., 2002). However, the precise roles of Shh signaling, such as the source and time of action for the patterning the forebrain, remain to be elucidated. Wnt signaling is also reported to be important for patterning of the forebrain along the anteroposterior (A–P) axis (Kim et al., 2000; Heisenberg et al., 2001). The first row of cells at the rostral margin of the neural plate were shown to pattern the anterior forebrain anteroposteriorly (Houart et al., 1998) and its function has been ascribed to the secretion of the Wnt antagonist, *tlc* (Houart et al., 2002), corroborating the importance of Wnt signaling for A–P patterning in the forebrain in zebrafish. Nevertheless, insights obtained from existing mutants are still fragmentary due to the limited number of mutants.

In vertebrates in which the functions of multiple genes often overlap, mutagenesis screens in a single species is not sufficient for uncovering all functioning genes in a genetic cascade or in the development of an organ, but this limitation should be largely alleviated by the use of another related animal species. Thus, to define the genetic components of the signaling required for patterning of the forebrain and their interplay, we have undertaken a large-scale mutagenesis screen in Medaka. Here, we report the initial characterization of 33 mutations in 25 complementation groups exhibiting specific defects in the development of the forebrain. These mutants show a reduction in the size of the telencephalon, and defects in the formation of the ventricle or axogenesis. These mutants are often phenotypically distinct from those of mutants isolated in zebrafish (Brand et al., 1996a,b; Furutani-Seiki et al., 1996; Heisenberg et al., 1996; Schier et al., 1996), supporting the importance of this fish species which complements zebrafish.

2. Results

2.1. Development and regionalization of forebrain in wild-type Medaka embryos

The forebrain formed at the most rostral portion of the neural plate is composed of the telencephalon and diencephalon, occupying its dorsoanterior and ventroposterior portions, respectively. In Medaka, the forebrain becomes distinguishable from the midbrain at the histological level at stage 19 (st. 19), 27 hours post fertilization (hpf) at 28 °C (Fig. 1A), (Iwamatsu, 1994), and morphologically at st. 21 (Fig. 1B). During st. 19 and 21, the tissue initially located at the rostral end of the brain tissue is displaced to the ventral side of the brain. At st. 23 (41 hpf), the forebrain ventricle starts to form (Fig. 1C). During st. 23 and st. 27, the initially linear anteroposterior (A–P) axis through the brain is bent in the diencephalon area forming the ventral diencephalon (hypothalamus) overlain by both the dorsal diencephalon and mesensephalon, thereby

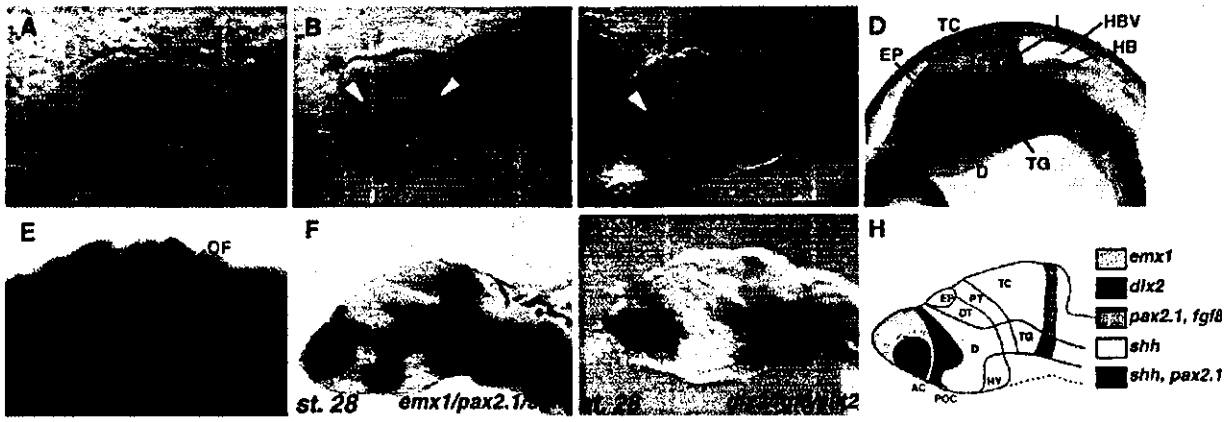

Fig. 1. Development and regionalization of the forebrain in wild-type Medaka embryos. (A–D) Morphology of the brain in Medaka live embryos. Dorsal view of wild-type embryo at (A) st. 19, (B) st. 21, (C) st. 23, (D) lateral view of the embryo at st. 27. (E) Major axonal scaffolds in the forebrain. Whole-mount immunostaining with anti-acetylated-tubulin and anti-HNK antibodies at st. 31. Ventral view of anterior portion of the head. (F,G) Whole-mount in situ hybridization analysis at st. 28. (F) *emx1*, *pax2.1*, *shh*; and (G) *dlx2*, *fgf8*, *slit2* as probes. (H) Schematic representation of gene expression patterns in subdivisions of the forebrain and midbrain. AC, anterior commissure; D, diencephalon; DT, dorsal thalamus; EP, epiphysis; F, forebrain; FV, forebrain ventricle; HB, hindbrain; HBV, hindbrain ventricle; HY, hypothalamus; I, isthmus; M, midbrain; OF, olfactory nerve; ON, optic nerve; POC, post-optic commissure; PT, pretectum; SOT, supraoptic tract; T, telencephalon; TC, tectum; TG, tegmentum; VT, ventral thalamus.

establishing the dorsoventral axis of the diencephalon (Fig. 1D). The cell layer of the roof of the telencephalon loses their thickness, and the telencephalon assumes its characteristic morphology. During st. 28–34 (64–131 hpf), cells proliferate extensively in the ventricular zone, and the ventricle loses its space (Ishikawa and Hyodo-Taguchi, 1994). The major axonal scaffolds in the forebrain, including commissural neurons, the supraoptic tract and sensory nerves, are formed by st. 34 (Fig. 1E).

In zebrafish, it was demonstrated that the expression patterns of marker genes define the transverse and longitudinal subdivisions within the forebrain and midbrain (Macdonald et al., 1994; Hauptmann and Gerster, 2000). Expression patterns of these markers seem to be well conserved in Medaka (Fig. 1F–H). For the initial characterization of Medaka forebrain mutants, we carried out whole-mount in situ hybridization analysis using a mixture of probes, *emx1/pax2.1/shh* and *dlx2/fgf8/slit2*. The dorsal and ventral telencephalon express *emx1* and *dlx2*, respectively. The diencephalon is divided into four domains; dorsal and ventral thalami, pretectum and hypothalamus. The zona limitans intrathalamica (zli), which expresses *shh*, divides the dorsal and ventral thalami. The ventral thalamus is marked by *dlx2* expression.

2.2. Identification of forebrain mutants in Medaka

Since a specific patterning defect often causes later occurrence of localized cell degeneration (Furutani-Seiki et al., 1996), we paid special attention to morphological abnormalities accompanied by cell degeneration. In the large-scale mutagenesis screen for embryonic pattern formation, we identified 33 mutations affecting forebrain development in Medaka mutants, exhibiting a variety of morphological defects and/or abnormal axonal pathways. These mutations were assigned to 25 complementation groups (Table 1). We classified these mutations into two groups, on the basis of the type of defects in the telencephalon. Class 1 mutations were those primarily affecting the size of the telencephalon, while Class 2 mutations were those mainly causing abnormalities in the forebrain shape without significantly affecting the size of the telencephalon. All the isolated mutations were zygotic recessive, and in this paper homozygous embryos are referred to as mutants. Two mutations turned out to be temperature sensitive; $kar^{j50\text{-}4A}$, which is sensitive to a low temperature (18 °C); and $ika^{j94\text{-}8A}$, which is sensitive to a high temperature (33 °C).

2.3. Class 1 mutations affecting telencephalon size

We have identified 15 mutations in 11 genes of this class causing reduction in telencephalon size (Fig. 2, arrowheads in A–F). According to the onset of the phenotype, we classified the Class 1 mutations into four subclasses, as summarized in Table 1.

2.3.1. Class 1A and 1B mutations affecting subregions of the telencephalon

In *kentoku* ($ket^{j23\text{-}3B}$) and *aonibi* ($aon^{j9\text{-}2F}$) mutant embryos, morphological defects appeared to be restricted to the telencephalon (Fig. 2B,C), whereas in *kobesshimi* ($kob^{j35\text{-}6D}$) and *bouzu* ($bou^{jr118\text{-}2A}$) mutant embryos, size reduction occurred also in the midbrain (Fig. 2D,E). On the other hand, *nopperabo* ($nop^{j80\text{-}19B}$) mutant embryos exhibited a characteristic phenotype, that is a reduction in forebrain size accompanied by the enlargement of the midbrain, reminiscent of that of *masterblind* (*mbl*) and *headless* (*hdl*) mutants in zebrafish (Fig. 2F).

Class 1 mutant embryos at st. 31 were immunochemically stained with anti-acetylated-tubulin and HNK1

Table 1
Mutations affecting formation of the forebrain

Gene	Symbol	Alleles	Forebrain phenotype	Other phenotypes
Class 1: mutations affecting the size of the telencephalon				
Class 1A: mutations affecting early specification of the telencephalon				
kentoku	*ket*	*j23-3B*	Telencephalon size reduced	
Class 1B: mutations affecting regionalization of the telencephalon				
aonibi	*aon*	*j9-2F, j60-3A*	Telencephalon size reduced	Lipid metabolism affected
kobesshimi	*kob*	*j9-10A, j35-6D, j54-3A*	Telencephalon size reduced	Midbrain slightly reduced
bouzu	*bou*	*jr118-2A*	Telencephalon size reduced	Midbrain anteroposteriorly reduced
nopperabo	*nop*	*j80-19B*	Telencephalon size reduced	Eyes missing, midbrain expanded
kumasaka	*kum*	*j54-20A*	Telencephalon size reduced	
usobuki	*uso*	*j14-26A*	Telencephalon size reduced	
Class 1C: a mutation affecting maintenance of the telencephalon				
hannya	*han*	*j41-3B*	Late telencephalon defect	–
Class 1D: mutations affecting formation of the midline neural tissue				
akatsuki	*aku*	*j22-15A, jf121-1A*	Telencephalon size reduced	Similar to zebrafish *oep*
akebono	*ake*	*j54-7A*	Telencephalon size reduced	Similar to zebrafish *oep*
mochizuki	*moc*	*j96-11B*	Telencephalon size reduced	Similar to zebrafish *oep*
Class 2: mutations affecting morphology of the telencephalon				
Class 2A: mutations affecting formation of the forebrain ventricle				
sarudahiko	*sar*	*j106-4A*	Forebrain ventricle reduced	Circulation, midline defect, tectum reduced
tengu	*ten*	*j2-11A, jr10-4D, j53-4C*	Forebrain ventricle reduced	Circulation, midline defect, tectum reduced
karuna	*kar*	*j50-4A*	Forebrain ventricle enlarged	Temperature sensitive at 18 °C
oobesshimi	*oob*	*j103-11A, j58-1A*	Forebrain ventricle enlarged	Tegmentum and hindbrain bumpy
samidare	*sam*	*j20-26A*	Forebrain ventricle enlarged	Similar to zebrafish *parachute* mutant
shigure	*sgu*	*j55-8A*	Forebrain ventricle enlarged	Similar to zebrafish *parachute* mutant
Class 2B: mutations affecting the formation of the anterior commissure				
ikazuchi	*ika*	*j94-8A*	Ectopic anterior commissure	Temperature sensitive at 33 °C, hindbrain bumpy
shikami	*shi*	*j92-3A*	Anterior commissure not formed	–
Class 2C: mutations causing forebrain dysmorphology				
baltan	*bal*	*j102-2A*	Forebrain dysmorphology, edema	Eyes small, tectum reduced, circulation defect, somite irregular
fukuwarai	*fuk*	*j8-33A, j93-4A*	Forebrain dysmorphology	Regions of CNS misplaced
yuzen	*yuz*	*j107-2D*	Forebrain dysmorphology	Regions of CNS misplaced
kagome	*kag*	*jr114-2D*	Forebrain dysmorphology	Regions of CNS misplaced
hirame	*hir*	*j54-20C*	Flattened, differentiation defect	CNS flat, heart beating next to ears
tobi	*tob*	*jr116-4A*	Protruding telencephalon	Eyes small

antibody to examine the paths and fasciculation of axons (Fig. 2G–L). In the wild type embryos, the olfactory nerve, anterior commissure, supraoptic tract and optic nerve were clearly stained (Fig. 2G). All Class 1 mutants showed interesting abnormalities in these nerves. In *ket* mutant embryos, anterior commissure nerves were not fully fasciculated (black arrowhead in Fig. 2H), displaced and lacked association with the olfactory nerve (white arrowheads in Fig. 2H), and the supraoptic tract was not clearly detected. In *aon* mutant embryos, the olfactory nerve and supraoptic tract were not detected, the anterior commissure lacked fasciculation (white arrowhead in Fig. 2I), and bundle formation of the optic nerve was also affected (black arrowhead in Fig. 2I). *kob* mutants were unique in that only olfactory nerve was affected and lacked fasciculation (arrowhead in Fig. 2J). In *bou* mutant embryos, the axons in the anterior commisure were totally defasciculated, and the commissure did not form (arrowhead in Fig. 2K). In the *nop* mutant embryos, all axonal paths were so severely affected and in astray that the nerves in the forebrain were not morphologically distinguishable each other (arrowhead in Fig. 2L). In addition, the olfactory bulbs appeared to be missing in *nop* mutant embryos (Fig. 2L). Thus, Class 1 mutants share the commonality of a reduced telencephalon size, but alterations of the nerves and their paths were affected distinctly.

Class 1 mutants were also examined for the regional markers of the forebrain by in situ hybridization with two sets of probes, *emx1/pax2.1/shh* and *dlx2/fgf8/slit2* (Fig. 2M–X). Consistent with a smaller telencephalon, Class 1 mutant embryos generally showed a reduction in *emx1* or *dlx2* expression in the telencephalon.

In *ket* and *nop* mutant embryos, the *emx1* expression was strongly reduced (black arrowhead in Fig. 2N,R) and

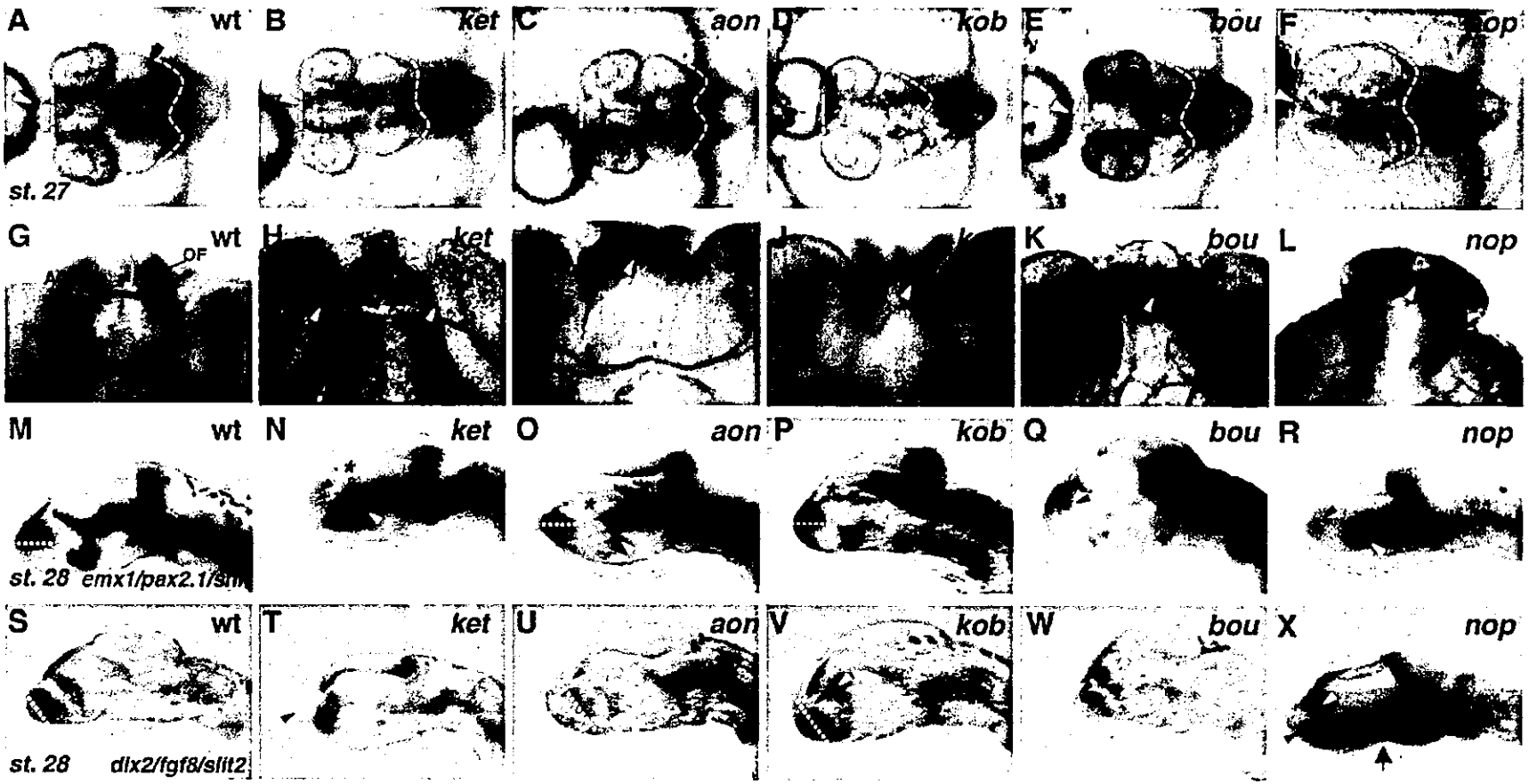

Fig. 2. Class 1 mutant phenotypes. (A,G,M,S) Wild type; (B,H,N,T) *ket*$^{j23\text{-}3B}$; (C,I,O,U) *aon*$^{j9\text{-}2F}$; (D,J,P,V) *kob*$^{j35\text{-}6D}$; (E,K,Q,W) *bou*$^{r118\text{-}2A}$; (F,L,R,X) *nop*$^{j80\text{-}19B}$ embryos. (A–F) Phenotypes of live Class 1 mutant embryos at st. 27 (dorsal view). White and black arrowheads indicate the positions of the telencephalon and midbrain, respectively. All Class 1 mutants show a reduction in the size of the telencephalon. Broken lines indicate the posterior edges of the telencephalon and the midbrain. (G–L) Whole-mount immuno-staining with anti-acetylated-tubulin and anti-HNK antibodies of embryos at st. 31. Ventral view of the anterior portion of the head. AC, anterior commissure; SOT, supraoptic tract; OF, olfactory nerve; ON, optic nerve. (M–X) In situ hybridization analysis of the forebrain of embryos at st 28. Lateral view of the head. (M–R) *emx1/pax2.1/shh*, and (S–X) *dlx2/fgf8/slit2* as probes, respectively.

the *dlx2* expression in the ventral telencephalon was almost absent (black arrowheads in Fig. 2T,X). In these mutants, the *shh* expression along the floor of the diencephalon (white arrowheads in Fig. 2N,R) dorsally expanded and, in *ket* mutant embryos, the expression in the zona limitans intrathalamica (zli) was lost (asterisk in Fig. 2N). The *dlx2* expression in the ventral thalamus showed an anterior shift (white arrowhead in Fig. 2T). In *nop* mutants, the *dlx2* expression marking the ventral thalamus anteriorly shifted, which was accompanied by the anterior expansion of the *dlx2* expression in the pharyngeal arch region (arrow in Fig. 2X).

In *aon* mutant embryos, the *emx1* expression shifted ventrally (broken line in Fig. 2M,O). Concomitantly, two domains of the *dlx2* expression in the ventral telencephalon and ventral thalamus shifted posteriorly (broken line in Fig. 2S,U to show the anterior limit of the *dlx2* expression; black and white arrowheads in Fig. 2U). The anteroventral region of the diencephalic *shh* expression was reduced (white arrowhead in Fig. 2O) and the *shh* expression in the zli was abolished (asterisk in Fig. 2O).

In *kob* mutants, the *emx1* expression shifted ventrally (broken line in Fig. 2P) and the *dlx2* expression in the ventral telencephalon shifted posteriorly (broken line and black arrowhead in Fig. 2V), and the *dlx2* expression in the ventral thalamus decreased (white arrowhead in Fig. 2V). *shh* expression in the zli and ventral diencephalon was low (asterisk and white arrowhead in Fig. 2P, respectively).

In *bou* mutant embryos, the *emx1* expression domain seems compressed anteroposteriorly (black arrowhead in Fig. 2Q) and the *dlx2* expression in the ventral thalamus became noncontinuous (white arrow head in Fig. 2W). The *shh* expression in the diencephalon was only rudimentary (white arrowhead in Fig. 2Q).

Thus, different patterning defects in the forebrain are included in these Class 1 mutants with smaller telencephalon. It is important to note that the majority of the mutants of this Class had an altered *shh* expression, particularly a reduction of *shh* expression in the zli.

2.3.2. Class 1A mutant kentoku representing an early fuction in telencephalon development

The expression of an early telencephalic marker *bf1* (Tao and Lai, 1992) was examined in all the Class 1 mutants. In wild-type Medaka embryos, *bf1* expression becomes detectable in the most anterior region of the brain at st. 19. *ket* mutant at st. 20 uniquely lacked the *bf1* expression (Fig. 3A,B). This observation indicated that *ket* is required in an early step in telencephalon development, possibly in the induction process. In *nop* mutant embryos, *bf1* expression was reduced at st. 20 probably due to the expansion of the diencephalon and mesencephalon at the expense of the telencephalon. In the rest of Class 1 mutants, *bf1* expression appeared normal (data not shown).

2.3.3. Class 1C mutation affecting maintenance of the telencephalon

In *hannya* (*han*$^{j41\text{-}3B}$) mutant embryos, the distance between the eyes decreased (arrow in Fig. 4A,E), but the floor plate was normal (data not shown), ruling out general midline defects. The expression of dorsal *emx1* was reduced in *han* mutant embryos (arrowheads in Fig. 4D,H). The projection pattern of trigeminal nerves was altered such that they did not extend toward the ventral surface of the forebrain at st. 31 (arrowheads in Fig. 4B,C,F,G). By contrast, the anterior commissure appeared normal. This phenotype was unique to *han* mutants and distinguished them from other Class 1 mutants.

2.3.4. Class 1D mutations exhibiting the phenotype similar to that of oep in zebrafish

The mutants of *akatsuki* (*aku*$^{j22\text{-}15A}$), *akebono*(*ake*$^{j54\text{-}7A}$) and *mochizuki*(*moc*$^{j96\text{-}11B}$), classified to 1D all displayed a drastic morphological phenotype similar to that of *one-eyed-pinhead* (*oep*) in zebrafish (Fig. 5A–D), where only one median eye was formed and the ventral brain tissue was severely affected. This phenotype was very similar to that of the zebrafish *oep* mutant (Schier et al., 1996). These three Medaka mutations sharing similar forebrain phenotypes complemented each other.

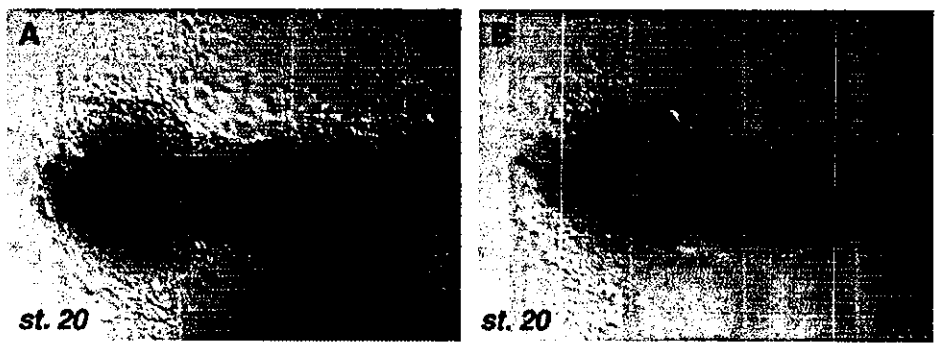

Fig. 3. Loss of *bf1* expression in *ket*$^{j23\text{-}3B}$ mutant embryo at st. 20. (A,B) Whole-mount in situ hybridization analysis of embryos at st. 20 with *bf1* probe. (A) Wild-type embryo. (B) *ket* mutant embryo.

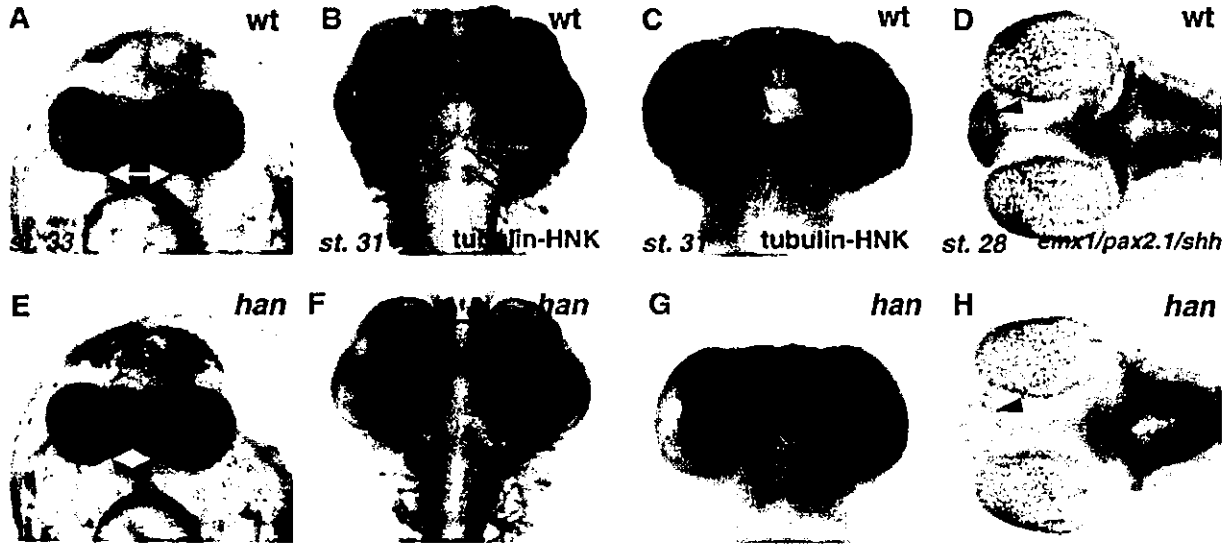

Fig. 4. *han*$^{j41\text{-}3B}$ mutant phenotypes. (A–D) wild type. (E–H) *han* mutant. (A,E) Live phenotype of embryos at st. 33. Anterior front view. Arrows show the width of the telencephalon. (B,C,F,G) Whole-mount staining of embryos at st. 31 with anti-acetylated-tubulin and HNK antibodies. (B,F) Ventral view; (C,G) Anterior front view. Arrowheads show the position of the trigeminal nerve. (D,H) Whole-mount in situ hybridization with *emx1/pax2.1/shh* probe mixture. Dorsal view of embryos at st. 28.

2.4. Class 2 mutations affecting the morphology of the forebrain

Class 2 mutations affecting forebrain shape without altering telencephalon size was divided into the subclasses, 2A to 2C, based on other associated phenotypes (Tables 1 and 2).

2.4.1. Class 2A mutations affecting the forebrain ventricle

We have identified mutations in 6 genes affecting the formation of the forebrain ventricle. In *sarudahiko* (*sar*$^{j106\text{-}4A}$) and *tengu* (*ten*$^{jr10\text{-}4D}$) mutant embryos, the ventricle of the forebrain did not inflate (arrowheads in Fig. 6A–C), the *emx1* expression did not extend ventrally as in the wild type (black arrowheads in Fig. 6P–R), while the *dlx2* expression remained normal (data not shown). It is remarkable that the *shh* expression in either the brain or the floor plate was absent, suggesting a defect in midline signaling (white arrowheads in Fig. 6Q,R). At the histological level, neuroepithelial cells in the forebrain and cortical layers of the retina were round and did not exhibit the characteristic polarized cell morphology (Fig. 6F–H,K–M). The defect at the cellular level may account for the defect in the histogenesis of the forebrain ventricle in these mutants. *sar* and *ten* mutants also shared a common defect in the cardiovascular system.

In *karuna* (*kar*$^{j50\text{-}4A}$) and *oobesshimi* (*oob*$^{j103\text{-}11A}$) mutant embryos, in contrast, the forebrain ventricle was abnormally expanded (arrowheads in Fig. 6A,D–F,I,J). *kar* mutant embryos also had small eyes (Fig. 6D,I), and a forebrain ventricle open on the ventral side (open arrowhead in Fig. 6I). The *shh* expression in the diencephalon was altered in *kar* mutant embryos (white and black arrowheads in Fig. 6S), suggesting that the patterning of the ventral forebrain is affected. In addition, the bilateral retinas were not completely separated in the midline (black arrowhead in Fig. 6I). It is interesting to determine whether this is caused by the altered development of the optic stalk or by a defect in the morphogenetic movement of diencephalon to split

Fig. 5. Mutants in 3 genes display phenotypes similar to that of *oep* zebrafish mutants. (A–D) Dorsal view of st. 27 live embryos of (A) wild-type; (B) *aku*$^{j22\text{-}15A}$ mutant; (C) *ake*$^{j54\text{-}7A}$ mutant and (D) *moc*$^{j96\text{-}11B}$ mutant.

Table 2
Defects in the axonal scaffolds and the gene expressions in the forebrain

Class	Genes	Structures									
		Anti-tubulin + HNK-1				*Emx1*	*Dlx2*		*Shh*		
		AC	SOT	OF	ON	dTel	vTel	vTha	Zli	vFor	Hth
Class 1A	*ket*	def	−	+	+	r	−	as	−	dve	ape
Class 1B	*aon*	def	−	−	+	vs	ps and r	ps and r	−	+	r
	kob	+	+	def	+	ve	ps and r	ps and r	r	r	+
	bou	def	−	def	def	apr	+	f	f	f	f
	nop	nj	nj	−	nj	r	−	as	−	+	pe
Class 2A	*sar*	nd	nd	nd	nd	de and vr	+	+	−	−	−
	ten	+	+	+	r	vr	+	+	−	−	−
	kar	nd	nd	nd	nd	ve	ps	ps and ve	+	+	r
	oob	nd	nd	nd	nd	+	ps and vr	ps and vr	r	r	r

AC, anterior commissure; For, forebrain; Hth, hypothalamus; OF, olfactory nerve; ON, optic nerve; SOT, supraoptic tract; Tel, telencephalon; Tha, thalamus; Zli, zona limitans intrathalamica; +, less affected; −, missing; r, reduced; e, expanded; s, shifted; f, fragmented; def, defasciculated; nj, not judgeable; nd, not done; a, anteriorly; p, posteriorly; d, dorsally; v, ventrally.

a single retinal field into bilateral optic primordia (Varga et al., 1999).

In *oob* mutant embryos, the enlarged ventricle could be observed from st. 25. The roof layer of the telencephalon appeared to be absent and the telencephalon became swollen at later stages (arrowhead in Fig. 6J). Despite the malformation of the forebrain ventricle, the cells in the neuroepithelium were normally polarized (Fig. 6J,O), and

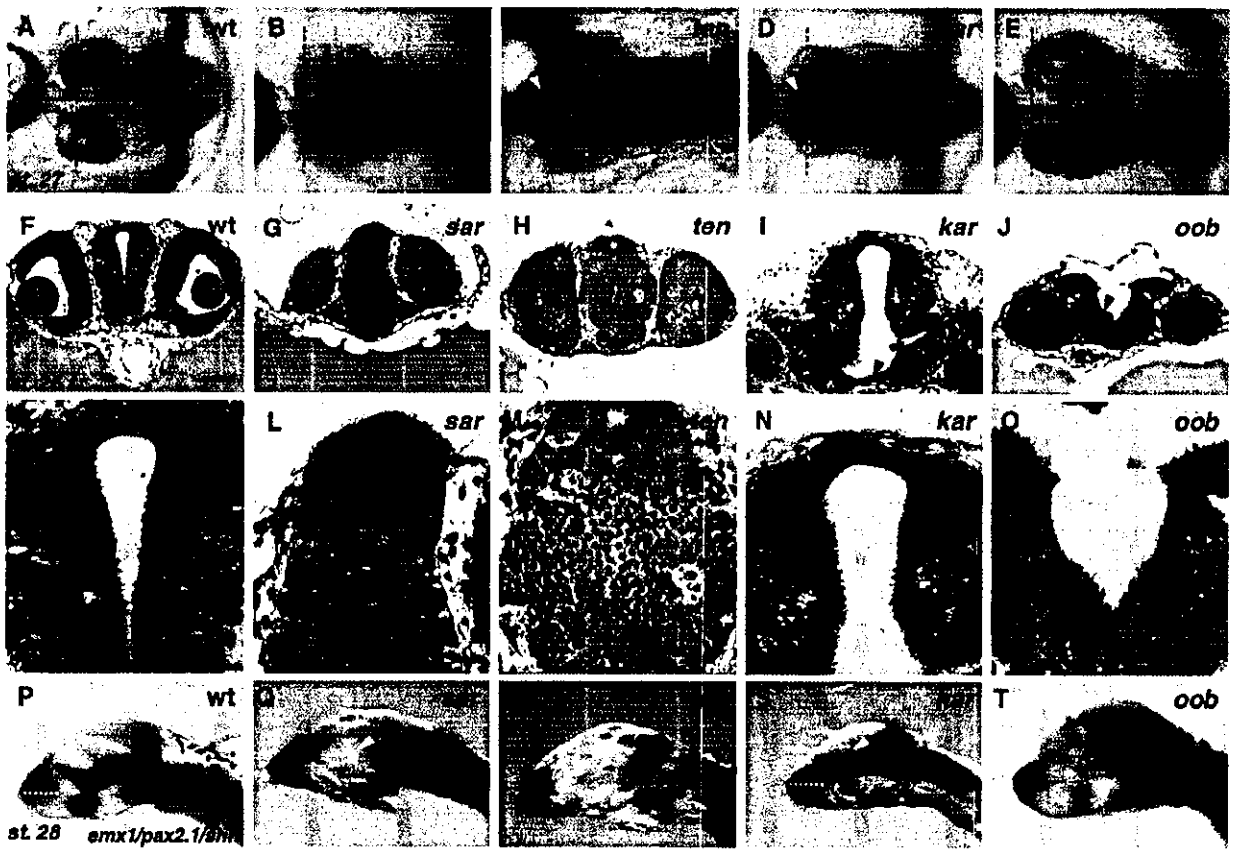

Fig. 6. Class 2A mutant phenotypes. (A,F,K,P) Wild type; (B,G,L,Q) *sar*$^{J106\text{-}4A}$; (C,H,M,R) *ten*$^{Jr10\text{-}4D}$; (D,I,N,S) *kar*$^{J50\text{-}4A}$; (E,J,O,T) *oob*$^{J103\text{-}11A}$ embryos. (A–E) Live phenotypes of Class 2A mutant embryos at st. 27 (dorsal view). Arrowheads show the forebrain ventricle. (F–J) Transverse sections of embryos at st. 26, stained with hematoxylin and eosin. (K–O) A higher magnification image of the transverse sections, focused on the cell layers around the forebrain ventricle. (P–T) Whole-mount in situ hybridization analysis of embryos at st. 28 with *emx1/pax2.1/shh* probe mixture. Lateral view of the brain. Scale bar, 50 μm.

the general pattern of gene expression was not significantly affected, except for the reduction in *shh* expression in the diencephalon (arrowhead in Fig. 6T).

2.4.2. Class 2B mutations affecting formation of anterior commissure

Anterior commissure nerves connect the two telencephalic hemispheres. We have identified two genes required for the formation of the commissure of bilateral axons from the dorsal telencephalon (Class 2B mutants).

In *shikami* (*shi*$^{j92\text{-}3A}$) mutant embryos, axons from the bilateral telencephalic halves did not associate with each other at the midline (arrowhead in Fig. 7D). Interestingly, it appears that axons originating from one side of the telencephalon crossed once to the other side then returned to the midline. The telencephalon tended to be distorted in *shi* mutant embryos (arrowhead in Fig. 7C).

In *ikazuchi* (*ika*$^{j94\text{-}8A}$) mutant embryos, axons from telencephalic clusters defasciculated and formed ectopic minor commissures in the dorsal telencephalon (arrowhead in Fig. 7F). The forebrain of *ika* was slightly enlarged (arrowhead in Fig. 7E).

2.4.3. The baltan mutation of Class 2D with a unique set of forebrain defects

baltan (*bal*$^{j102\text{-}2A}$) mutant embryos were recognized by an early focal neural degeneration in the forebrain, leading to a reduction of the forebrain size and an edema (Fig. 8A,G). Surprisingly, staining of axons of cranial nerves revealed that many axons crossed the midline at various A–P levels, causing a ladderlike appearance (arrowheads in Fig. 8B,H). The bilateral optic nerve did not form a chiasm between the eyes but crossed the midline at the anterior commissure (arrowheads in Fig. 8C,I). The *emx1* expression was absent and the *dlx2* expression in the ventral telencephalon was attenuated (black arrowheads in Fig. 8D,E,J,K). *dlx2* expression in the ventral thalamus was markedly reduced (white arrowheads in Fig. 8E,K), suggesting a seriously defective regionalization of the forebrain in the *baltan*

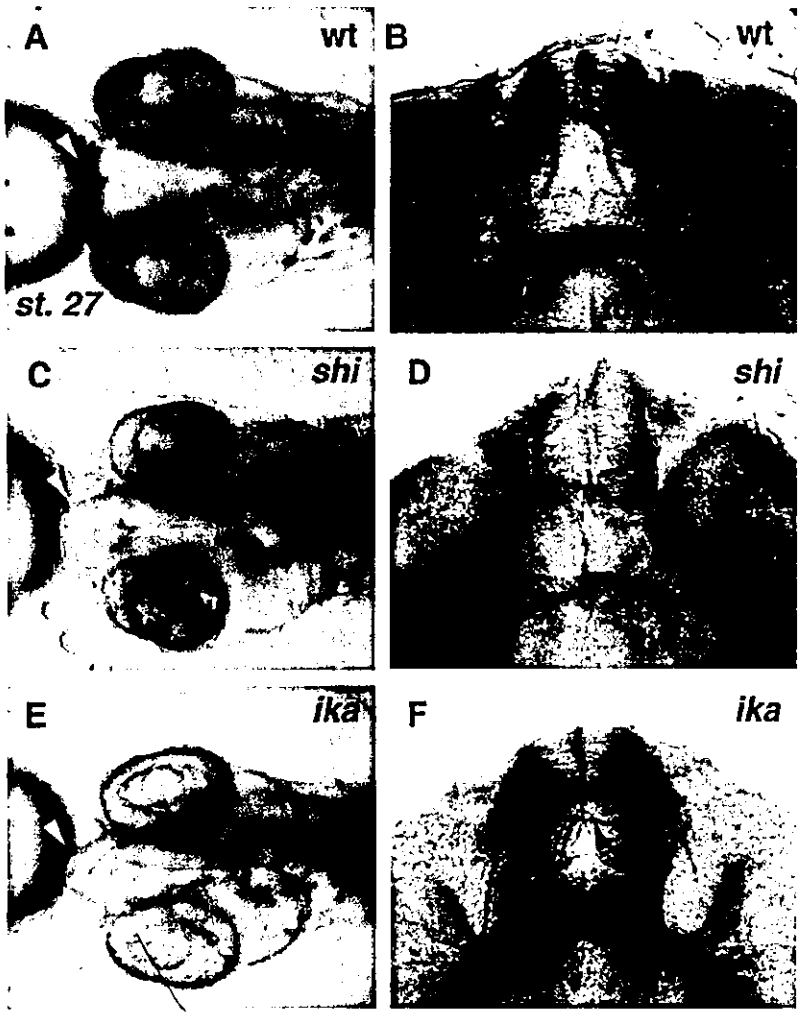

Fig. 7. Class 2B mutant phenotypes. (A,B) wild type; (C,D) *shi*$^{j92\text{-}3A}$; (E,F) *ika*$^{j94\text{-}8A}$. (A,C,E) Morphology of Class 2B mutant embryos at st. 27 (dorsal view). (B,D,F) Whole-mount staining of embryos at st. 31 with anti-acetylated-tubulin and HNK antibodies. Arrowheads show the anterior commissure.

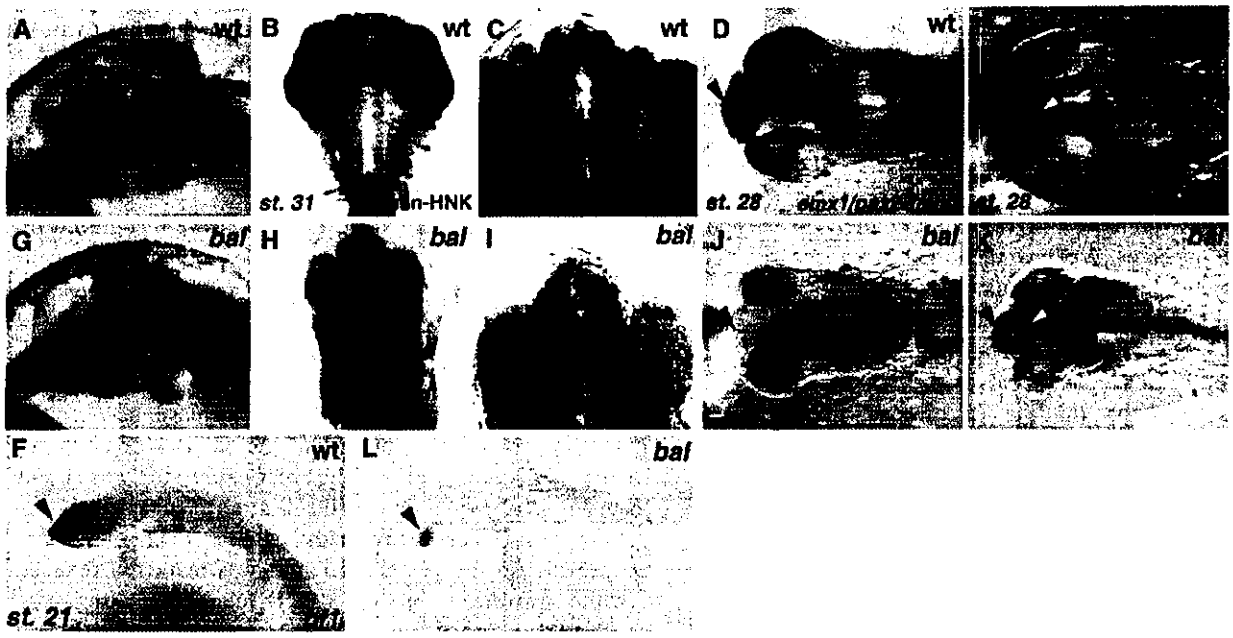

Fig. 8. *bal*$^{102\text{-}2A}$ mutant phenotypes. (A–F) Wild type; (G–L) *bal*$^{102\text{-}2A}$ embryos. (A,G) Live embryos of wild-type (A) and (G) *bal*$^{102\text{-}2A}$ mutant at st. 30 (lateral view). An arrowhead in G shows an empty space generated by degeneration in the forebrain. (B,C,H,I) Whole-mount immunostaining of st. 31 embryos using anti-acetylated tubulin and HNK antibodies. (B,H) Ventral view of the head. An arrowhead indicates ladder like axons of unknown origin. (C,I) enlarged view of (B,H). an arrowhead shows the optic nerve. (D–F,J–L) Whole-mount in situ hybridization analysis of embryos at st.28 (D,E,J,K, dorsal view) and st.21 (F,L, lateral view), using (D,J) *emx1/pax2.1/shh*; (E,K) *dlx2/fgf8/slit2* and (F,L) *bf1* as probes. (F,L) Arrowheads indicate the *bf1* expression in the telencephalon.

mutant. Moreover, *bf1* expression at the induction phase of telencephalon was remarkably reduced (Fig. 8F,L). These results suggested that *bal* is necessary for early specification of the forebrain as well as proper axonal projection of cranial nerves.

3. Discussion

3.1. Class 1 mutations causing smaller telencephalon

ket mutants are remarkable for their compromised expression of the early telencephalon marker *bf1*(Fig. 3). In parallel, both *emx1* expression in the dorsal telencephalon and the *dlx2* expression in the ventral telencephalon are strongly reduced, raising the possibility that *ket* is a key regulator required for specification of the telencephalon (Fig. 2N,T). The phenotype of *ket* mutants is reminiscent of that of the *bf1* knockout mouse with hypoplasia of the cerebral hemispheres and more severe defects in the basal region of the telencephalon (Dou et al., 1999). The expression of both *bf1* and *emx1* is reduced in *tlc*-knockdown embryos after the injection of antisense morpholino oligonucleotides (Houart et al., 2002). The possible genetic linkage of *ket* with *bf1* and *tlc* is currently under investigation. In mice, Fgf8 induces *bf1* expression under in vitro culture condition of the forebrain tissue (Shimamura and Rubenstein, 1997). However, telencephalon is somehow formed in the *fgf8* mutants of mice and zebrafish, suggesting it alone is not responsible for induction of the telencephalon (Meyers et al., 1998; Reifers et al., 1998; Shanmugalingam et al., 2000; Shinya et al., 2001).

The major feature of *aon* and *kob* mutants is their defect in dorsoventral (D–V) patterning in the telencephalon. The tissue area for *emx1* expression in the dorsal telencephalon expands or shifts ventrally, and the *dlx2* expression in the ventral telencephalon is reduced and posteriorly displaced (Fig. 2O,P,U,V).

shh-null mice lack any signs of the medial ganglionic eminence (MGE), which is the ventral portion of the basal ganglia, indicating that Shh is required for the patterning of the ventral telencephalon (Chiang et al., 1996). However, it is yet to be determined which part of *shh* expression in the forebrain is required for the D–V patterning of the telencephalon. All the Class 1 mutants have an altered *shh* expression, particularly in the zli (Fig. 2N–R). The zli not only forms a clear histological border between the dorsal and ventral thalami (Larsen et al., 2001), but, for its *shh* expression, is considered to function as a secondary organizing center. The presence of patterning defects of the telencephalon in Class 2 mutants corroborates this notion.

It is to be noted that the phenotype of the Class 1 mutants associated with the decreased expression of *shh* in the forebrain does not resemble those of zebrafish mutants defective in sonic hedgehog signaling, *sonic you* (*syu*),

detour (*dtr*), *you-too* (*yot*) and *slow-muscle-omitted* (*smu*), in which *shh, gli1, gli2, foxh1* and *smoothened*, respectively, are mutated and the primary causes are defects in the midline tissues (Schauerte et al., 1998; Karlstrom et al., 1999; Barresi et al., 2000; Chen et al., 2001; Varga et al., 2001; Karlstrom et al., 2003).

The phenotype of the *nop* mutant, characterized by the expansion of the diencephalon and mesencephalon at the expense of the telencephalon tissue (Fig. 2F), is reminiscent of those of *masterblind(mbl)* and *headless* (*hdl*) mutants of zebrafish. In these zebrafish mutants, the genes coding for the negative regulators of Wnt signaling, *tcf3* and *axin1*, respectively, are mutated, possibly resulting in the over-activation of Wnt signaling throughout the forebrain (Kim et al., 2000; Heisenberg et al., 2001). It is also known that a secreted Wnt antagonist *tlc* is expressed in the anterior neural ridge (Houart et al., 2002). Whether the *nop* gene function is involved in Wnt signaling is of an immediate interest.

3.2. Patterning defects resulting in defective formation of forebrain ventricle

sar and *ten* mutants lack polarized cell shape in the neuroepithelium on one hand (Fig. 6L,M), and show an attenuated *shh* expression in the forebrain and spinal cord on the other (Fig. 6Q,R). It is currently under investigation how these phenotypes correlate with each other.

In *oob* mutants showing the expansion of the forebrain ventricle, the roof plate is missing and the basal plate is thicker (Fig. 6J). This phenotype may reflect an altered D–V patterning or a defect in the histogenetic process dependent on cell–cell interactions. It is interesting to note that the phenotype of *oob* mutants somewhat resembles that of the zebrafish *parachute* mutant of the N-cadherin gene (Lele et al., 2002; Erdmann et al., 2003).

3.3. Mutations affecting axonal paths in the forebrain

Class 2B mutants have characteristic defects in the formation of the anterior commissure. Interestingly, the formation of the anterior commissure is affected differently in *shi* and *ika* mutants, suggesting that *shi* and *ika* may be required for a distinct process in anterior commissure formation (Fig. 7).

It is suggested in zebrafish that a commissure is formed through three steps (Bak and Fraser, 2003). The first step is the extension of the leader axon toward the midline through the already defined axonal tract. The growth cone senses and integrates attractive and repulsive midline cues for their behavior. The second step is the growth and extension of the follower axon along the leader axon toward the midline and its fasciculation with the leader axon. The third step is the interaction of the axons with the leader axon of the opposite side across the midline and mutual fasciculation. In this way, the leader axons from two sides cooperate with each other to establish a commisure across the midline.

In *ika* mutants, the first step may be disturbed since the anterior commisure was formed but in an ectopic position (Fig. 7F). The group of Class 1 mutants, *bou, ket* and *aon*, may have a defect in the second step. The failure of the axons to properly cross the midline in *bou* mutants may be explained by the loss of interaction between the leader and follower axons (Fig. 2K). In *ket* and *aon* mutants, a mild defasciculation of axons in the anterior commissure was observed (Fig. 2H,I).

In *bal* mutants, the anterior commissure and optic nerve joined together. In the region between the anterior commissure and the optic nerve, Netrins, the repulsive cues for axons, are known to be expressed. Indeed, the *netrin* expression in this region was altered in *noi* and *ace* zebrafish mutant embryos, accompanied by abnormalities of the anterior and postoptic commissures (Macdonald et al., 1997; Shanmugalingam et al., 2000). It would be interesting to determine whether the *netrin* expression between the anterior commissure and the optic nerve is altered in *bal* mutants. In *shi* mutants, the third step may be affected, since the commissure structure crossing the midline was not established.

In the Class 1 mutants which have altered gene expression pattern, the formation of axonal scaffolds in the forebrain is also affected, as summarized in Table 2. In zebrafish, the boundaries of regulatory gene expression domains correspond in many cases to early axonal scaffolds in the forebrain (Macdonald et al., 1994). It has been hypothesized that a growth cone extends along the interface between two domains of cells with different cell surface properties. Class 1 Medaka mutants should prove useful in testing this hypothesis.

3.4. Medaka and zebrafish complement to genetically dissect forebrain formation

We have identified 25 loci required for the formation of the forebrain in the systematic screen in Medaka. Although screenings covering the whole genome have already been carried out in zebrafish, we identified a battery of mutations resulting in phenotypes that were not observed in the zebrafish mutant collection. This could reflect (1) the difference in the functional overlap of genes, (2) the difference in the regulation of forebrain development, (3) the difference in susceptibility to mutagens of a genetic locus between Medaka and zebrafish.

Some other mutant phenotypes corresponded to those of identified zebrafish mutants. These mutated genes of shared phenotypes must be involved in the genetic pathways conserved between the two species. Interestingly, mutations in 3 genes, *aku, ake* and *moc* of Class 1D result in a phenotype similar to that of *one-eyed-pinhead* (*oep*) in zebrafish (Schier et al., 1997; Strahle et al., 1997). In zebrafish, mutants of other genes involved in Nodal

signaling, *cyclops(cyc)*, *squint* (*sqt*), and *schmalspur* (*sur*) displayed slightly different phenotypes, suggesting a divergence of the molecular components in a signaling pathway between the two species (Hatta et al., 1994; Brand et al., 1996b; Malicki et al., 1996; Schier et al., 1996; Heisenberg and Nusslein-Volhard, 1997; Feldman et al., 1998; Rebagliati et al., 1998; Sampath et al., 1998; Pogoda et al., 2000; Sirotkin et al., 2000). Similarly, mutations in 3 genes, *oob*, *sam*, and *sgu*, caused phenotypes that are reminiscent of those of *parachute* zebrafish mutant of the N-cadherin gene. No mutations in other genes are reported in zebrafish to cause the *parachute* phenotype (Lele et al., 2002; Erdmann et al., 2003). Cloning of these mutated genes in Medaka and the analysis of their function will reveal both conserved and divergent functions of the genes essential for forebrain formation. The results of the mutant screen in Medaka do demonstrate that zebrafish and Medaka complement each other in uncovering more genes and more functions involved in the developmental process.

4. Experimental procedures

4.1. Mutant embryos

Fish are mutagenized and screened for mutations as described in an accompanying paper (Furutani-Seiki et al., this issue). Mutant embryos were obtained by mating heterozygotes, reared at 28 °C, and staged according to the development of sibling normal embryos. Live embryos were photographed after removing the chorion and mounting in 2.5% methylcellulose.

4.2. Histological methods

Whole-mount staining of the embryos by in situ hybridization or with anti-acetylated tubulin/anti-HNK1 antibodies was performed as described by Hammerschmidt and Nusslein-Volhard (1993). RNA probes for in situ hybridization were labeled with digoxygenin, and detected using an anti-digoxygenin antibody conjugated with alkalinephophatase, and reacted with BM purple (Roche) for color development. For histological sections, the embryos were fixed in 4% paraformaldehyde, dehydrated through ethanol series and embedded in Jung HistoResin Plus (Leica) and sections 4 μm thickness of were made.

Acknowledgements

We are grateful to Dr Giselbert Hauptmann for input about regionalization of medaka brain, Drs Takashi Sasaki and Noboru Nakajima for cloning *slit2*, *dlx2* and *bf1* probes. This work was supported by the ERATO project of the Japan Science and Technology Agency to H.K.

References

Bak, M., Fraser, S.E., 2003. Axon fasciculation and differences in midline kinetics between pioneer and follower axons within commissural fascicles. Development 130, 4999–5008.

Barresi, M.J., Stickney, H.L., Devoto, S.H., 2000. The zebrafish slow-muscle-omitted gene product is required for Hedgehog signal transduction and the development of slow muscle identity. Development 127, 2189–2199.

Brand, M., Heisenberg, C.P., Jiang, Y.J., Beuchle, D., Lun, K., Furutani-Seiki, M., et al., 1996a. Mutations in zebrafish genes affecting the formation of the boundary between midbrain and hindbrain. Development 123, 179–190.

Brand, M., Heisenberg, C.P., Warga, R.M., Pelegri, F., Karlstrom, R.O., Beuchle, D., et al., 1996b. Mutations affecting development of the midline and general body shape during zebrafish embryogenesis. Development 123, 129–142.

Bulfone, A., Puelles, L., Porteus, M.H., Frohman, M.A., Martin, G.R., Rubenstein, J.L., 1993. Spatially restricted expression of Dlx-1, Dlx-2 (Tes-1), Gbx-2, and Wnt-3 in the embryonic day 12.5 mouse forebrain defines potential transverse and longitudinal segmental boundaries. J. Neurosci. 13, 3155–3172.

Chen, W., Burgess, S., Hopkins, N., 2001. Analysis of the zebrafish smoothened mutant reveals conserved and divergent functions of hedgehog activity. Development 128, 2385–2396.

Chiang, C., Litingtung, Y., Lee, E., Young, K.E., Corden, J.L., Westphal, H., Beachy, P.A., 1996. Cyclopia and defective axial patterning in mice lacking Sonic hedgehog gene function. Nature 383, 407–413.

Dou, C.L., Li, S., Lai, E., 1999. Dual role of brain factor-1 in regulating growth and patterning of the cerebral hemispheres. Cereb. Cortex 9, 543–550.

Erdmann, B., Kirsch, F.P., Rathjen, F.G., More, M.I., 2003. N-cadherin is essential for retinal lamination in the zebrafish. Dev. Dyn. 226, 570–577.

Feldman, B., Gates, M.A., Egan, E.S., Dougan, S.T., Rennebeck, G., Sirotkin, H.I., et al., 1998. Zebrafish organizer development and germ-layer formation require nodal-related signals. Nature 395, 181–185.

Fernandez, A.S., Pieau, C., Reperant, J., Boncinelli, E., Wassef, M., 1998. Expression of the Emx-1 and Dlx-1 homeobox genes define three molecularly distinct domains in the telencephalon of mouse, chick, turtle and frog embryos: implications for the evolution of telencephalic subdivisions in amniotes. Development 125, 2099–2111.

Figdor, M.C., Stern, C.D., 1993. Segmental organization of embryonic diencephalon. Nature 363, 630–634.

Furutani-Seiki, M., Jiang, Y.J., Brand, M., Heisenberg, C.P., Houart, C., Beuchle, D., et al., 1996. Neural degeneration mutants in the zebrafish, *Danio rerio*. Development 123, 229–239.

Hatta, K., Puschel, A.W., Kimmel, C.B., 1994. Midline signaling in the primordium of the zebrafish anterior central nervous system. Proc. Natl Acad. Sci. USA 91, 2061–2065.

Hauptmann, G., Gerster, T., 2000. Regulatory gene expression patterns reveal transverse and longitudinal subdivisions of the embryonic zebrafish forebrain. Mech. Dev. 91, 105–118.

Hauptmann, G., Soll, I., Gerster, T., 2002. The early embryonic zebrafish forebrain is subdivided into molecularly distinct transverse and longitudinal domains. Brain Res. Bull. 57, 371–375.

Heisenberg, C.P., Nusslein-Volhard, C., 1997. The function of silberblick in the positioning of the eye anlage in the zebrafish embryo. Dev. Biol. 184, 85–94.

Heisenberg, C.P., Brand, M., Jiang, Y.J., Warga, R.M., Beuchle, D., van Eeden, F.J., et al., 1996. Genes involved in forebrain development in the zebrafish, *Danio rerio*. Development 123, 191–203.

Heisenberg, C.P., Houart, C., Take-Uchi, M., Rauch, G.J., Young, N., Coutinho, P., et al., 2001. A mutation in the Gsk3-binding domain of zebrafish Masterblind/Axin1 leads to a fate transformation of telencephalon and eyes to diencephalon. Genes Dev. 15, 1427–1434.

Houart, C., Westerfield, M., Wilson, S.W., 1998. A small population of anterior cells patterns the forebrain during zebrafish gastrulation. Nature 391, 788–792.

Houart, C., Caneparo, L., Heisenberg, C., Barth, K., Take-Uchi, M., Wilson, S., 2002. Establishment of the telencephalon during gastrulation by local antagonism of Wnt signaling. Neuron 35, 255–265.

Ishikawa, Y., Hyodo-Taguchi, Y., 1994. Cranial nerves and brain fiber systems of the medaka fry as observed by a whole-mount staining method. Neurosci. Res. 19, 379–386.

Iwamatsu, T., 1994. Stages of normal development in the medaka *Oryzias latipes*. Zool. Sci. 11, 825–839.

Karlstrom, R.O., Talbot, W.S., Schier, A.F., 1999. Comparative synteny cloning of zebrafish you-too: mutations in the Hedgehog target gli2 affect ventral forebrain patterning. Genes Dev. 13, 388–393.

Karlstrom, R.O., Tyurina, O.V., Kawakami, A., Nishioka, N., Talbot, W.S., Sasaki, H., Schier, A.F., 2003. Genetic analysis of zebrafish gli1 and gli2 reveals divergent requirements for gli genes in vertebrate development. Development 130, 1549–1564.

Kim, C.H., Oda, T., Itoh, M., Jiang, D., Artinger, K.B., Chandrasekharappa, S.C., et al., 2000. Repressor activity of Headless/Tcf3 is essential for vertebrate head formation. Nature 407, 913–916.

Larsen, C.W., Zeltser, L.M., Lumsden, A., 2001. Boundary formation and compartition in the avian diencephalon. J. Neurosci. 21, 4699–4711.

Lele, Z., Folchert, A., Concha, M., Rauch, G.J., Geisler, R., Rosa, F., et al., 2002. parachute/n-cadherin is required for morphogenesis and maintained integrity of the zebrafish neural tube. Development 129, 3281–3294.

Macdonald, R., Xu, Q., Barth, K.A., Mikkola, I., Holder, N., Fjose, A., et al., 1994. Regulatory gene expression boundaries demarcate sites of neuronal differentiation in the embryonic zebrafish forebrain. Neuron 13, 1039–1053.

Macdonald, R., Scholes, J., Strahle, U., Brennan, C., Holder, N., Brand, M., Wilson, S.W., 1997. The Pax protein Noi is required for commissural axon pathway formation in the rostral forebrain. Development 124, 2397–2408.

Malicki, J., Neuhauss, S.C., Schier, A.F., Solnica-Krezel, L., Stemple, D.L., Stainier, D.Y., et al., 1996. Mutations affecting development of the zebrafish retina. Development 123, 263–273.

Mathieu, J., Barth, A., Rosa, F.M., Wilson, S.W., Peyrieras, N., 2002. Distinct and cooperative roles for Nodal and Hedgehog signals during hypothalamic development. Development 129, 3055–3065.

Meyers, E.N., Lewandoski, M., Martin, G.R., 1998. An Fgf8 mutant allelic series generated by Cre- and Flp-mediated recombination. Nat. Genet. 18, 136–141.

Pogoda, H.M., Solnica-Krezel, L., Driever, W., Meyer, D., 2000. The zebrafish forkhead transcription factor FoxH1/Fast1 is a modulator of nodal signaling required for organizer formation. Curr. Biol. 10, 1041–1049.

Puelles, L., Rubenstein, J.L., 1993. Expression patterns of homeobox and other putative regulatory genes in the embryonic mouse forebrain suggest a neuromeric organization. Trends Neurosci. 16, 472–479.

Puelles, L., Kuwana, E., Puelles, E., Bulfone, A., Shimamura, K., Keleher, J., et al., 2000. Pallial and subpallial derivatives in the embryonic chick and mouse telencephalon, traced by the expression of the genes Dlx-2, Emx-1, Nkx-2.1, Pax-6, and Tbr-1. J. Comp. Neurol. 424, 409–438.

Rallu, M., Corbin, J.G., Fishell, G., 2002. Parsing the prosencephalon. Nat. Rev. Neurosci. 3, 943–951.

Rebagliati, M.R., Toyama, R., Haffter, P., Dawid, I.B., 1998. Cyclops encodes a nodal-related factor involved in midline signaling. Proc. Natl Acad. Sci. USA 95, 9932–9937.

Reifers, F., Bohli, H., Walsh, E.C., Crossley, P.H., Stainier, D.Y., Brand, M., 1998. Fgf8 is mutated in zebrafish acerebellar (ace) mutants and is required for maintenance of midbrain–hindbrain boundary development and somitogenesis. Development 125, 2381–2395.

Rohr, K.B., Barth, K.A., Varga, Z.M., Wilson, S.W., 2001. The nodal pathway acts upstream of hedgehog signaling to specify ventral telencephalic identity. Neuron 29, 341–351.

Sampath, K., Rubinstein, A.L., Cheng, A.M., Liang, J.O., Fekany, K., Solnica-Krezel, L., et al., 1998. Induction of the zebrafish ventral brain and floorplate requires cyclops/nodal signalling. Nature 395, 185–189.

Schauerte, H.E., van Eeden, F.J., Fricke, C., Odenthal, J., Strahle, U., Haffter, P., 1998. Sonic hedgehog is not required for the induction of medial floor plate cells in the zebrafish. Development 125, 2983–2993.

Schier, A.F., Neuhauss, S.C., Harvey, M., Malicki, J., Solnica-Krezel, L., Stainier, D.Y., et al., 1996. Mutations affecting the development of the embryonic zebrafish brain. Development 123, 165–178.

Schier, A.F., Neuhauss, S.C., Helde, K.A., Talbot, W.S., Driever, W., 1997. The one-eyed pinhead gene functions in mesoderm and endoderm formation in zebrafish and interacts with no tail. Development 124, 327–342.

Shanmugalingam, S., Houart, C., Picker, A., Reifers, F., Macdonald, R., Barth, A., et al., 2000. Ace/Fgf8 is required for forebrain commissure formation and patterning of the telencephalon. Development 127, 2549–2561.

Shimamura, K., Rubenstein, J.L., 1997. Inductive interactions direct early regionalization of the mouse forebrain. Development 124, 2709–2718.

Shinya, M., Koshida, S., Sawada, A., Kuroiwa, A., Takeda, H., 2001. Fgf signalling through MAPK cascade is required for development of the subpallial telencephalon in zebrafish embryos. Development 128, 4153–4164.

Sirotkin, H.I., Gates, M.A., Kelly, P.D., Schier, A.F., Talbot, W.S., 2000. Fast1 is required for the development of dorsal axial structures in zebrafish. Curr. Biol. 10, 1051–1054.

Strahle, U., Jesuthasan, S., Blader, P., Garcia-Villalba, P., Hatta, K., Ingham, P.W., 1997. One-eyed pinhead is required for development of the ventral midline of the zebrafish (*Danio rerio*) neural tube. Genes Funct. 1, 131–148.

Tao, W., Lai, E., 1992. Telencephalon-restricted expression of BF-1, a new member of the HNF-3/fork head gene family, in the developing rat brain. Neuron 8, 957–966.

Varga, Z.M., Wegner, J., Westerfield, M., 1999. Anterior movement of ventral diencephalic precursors separates the primordial eye field in the neural plate and requires cyclops. Development 126, 5533–5546.

Varga, Z.M., Amores, A., Lewis, K.E., Yan, Y.L., Postlethwait, J.H., Eisen, J.S., Westerfield, M., 2001. Zebrafish smoothened functions in ventral neural tube specification and axon tract formation. Development 128, 3497–3509.

Wilson, S.W., Rubenstein, J.L., 2000. Induction and dorsoventral patterning of the telencephalon. Neuron 28, 641–651.

JB Minireview

J. Biochem. **136**, 00–00 (2004)
DOI: 10.1093/jb/mvh117

Physiological Roles of SAPK/JNK Signaling Pathway

Hiroshi Nishina*, Teiji Wada and Toshiaki Katada

Department of Physiological Chemistry, Graduate School of Pharmaceutical Sciences, University of Tokyo, Tokyo 113-0033

Received May 6, 2004; accepted May 6, 2004

Stress-activated protein kinase/c-Jun NH_2-terminal kinase (SAPK/JNK) is activated by many types of cellular stresses and extracellular signals. Recent studies, including the analysis with knockout mice, have led to progress towards understanding the physiological roles of SAPK/JNK activation in embryonic development in addition to immune responses. SAPK/JNK activation plays essential roles in organogenesis during mouse development by regulating cell survival, apoptosis, and proliferation. Two SAPK/JNK activators, SEK1 and MKK7, are required for fetal liver formation and full activation of SAPK/JNK, which responds to various stimuli in an all-or-none manner. This article focuses on physiological roles of SAPK/JNK activation in fetal liver formation and in apoptosis regulation.

Key words: apoptosis, liver formation, MAP kinase, SAPK/JNK, stress.

Developmental programs and environmental agents trigger distinct and evolutionarily conserved kinases that relay signals mediating survival, death, proliferation, and cell cycle arrest. Mitogen-activated protein kinases (MAPKs) are evolutionarily conserved serine/threonine kinases involved in regulation of many cellular events. Several MAPK groups have been identified in mammalian cells, including extracellular signal-regulated kinase (ERK), p38, and SAPK/JNK. These MAPKs are activated by their specific MAPK kinases (MAPKKs): ERK by MEK1 and MEK2, p38 by MKK3 and MKK6, and SAPK/JNK by SEK1 (also known as MKK4) and MKK7 (SEK2). These MAPKKs are also activated by various MAPKK kinases (MAPKKKs) such as Raf, MLK, MEKK1, TAK1, and ASK1.

SAPK/JNK is ubiquitously expressed and is activated by many types of stress, including UV and γ-irradiation, protein synthesis inhibitors (anisomycin), hyperosmolarity, toxins, ischemia/reperfusion injury in heart attacks, heat shock, anticancer drugs (cisplatinum, adriamycin, or etoposide), ceramide, T-cell receptor stimulation, peroxide, and inflammatory cytokines such as TNFα. Recently, several *in vitro* and *in vivo* experiments have shown that SAPK/JNK is activated synergistically by SEK1 and MKK7. The SAPK/JNK stress pathway participates in many different intracellular signaling pathways that control a spectrum of cellular processes, including cell proliferation, differentiation, transformation, apoptosis, migration, and cytoskeletal integrity. SAPK/JNK has been reported to phosphorylate transcription factors in addition to c-Jun, such as ATF-2, Elk-1, p53, and c-Myc, as well as nontranscription factors such as Bcl-2, Bcl-xL, paxillin, and MAP2 (*1–6*). This review summarizes recent progress in the SAPK/JNK signaling pathway in mouse development and the molecular mechanism of SAPK/JNK activation.

*To whom correspondence should be addressed. Tel: +81-3-5841-4754, Fax: +81-3-5841-4751, E-mail: nishina@mol.f.u-tokyo.ac.jp

Role of SAPK/JNK in mouse development

All three *Jnk* (*Jnk1, 2,* and *3*), and *sek1* and *mkk7* loci have been knocked out. JNK1 and JNK2 are widely expressed in many tissues, but JNK3 is expressed predominantly in nervous system. Mice deficient in the single gene of *Jnk1*, *Jnk2*, or *Jnk3*, and *Jnk1/Jnk3*– or *Jnk2/Jnk3*–double mutant mice all survived normally. Mice lacking both JNK1 and JNK2 die around embryonic day 11 (E11) with severe dysregulation of apoptosis in the brain (*7, 8*). Specifically, there was a reduction of cell death in the lateral edges of the hindbrain prior to neural tube closure. In contrast, increased apoptosis and caspase activation were found in the mutant forebrain. These results assign both pro-and anti-apoptotic functions to JNK1 and JNK2 in the development of the fetal brain.

Sek1$^{-/-}$ embryos die between E10.5 and E12.5 with impaired liver formation and massive apoptosis (*9–12*). We have recently shown that SEK1-mediated SAPK/JNK pathway downstream TNF-α receptor 1 (TNFR1) participates in embryonic hepatoblast proliferation and survival via a pathway different from NF-κB–induced anti-apoptosis (*13*). Furthermore, *mkk7*$^{-/-}$ embryos die between E11.5 and E12.5 with similar defects in liver formation (*14*). These results indicate that SEK1 and MKK7 cannot substitute for one another *in vivo* and that both are important for hepatoblast proliferation and survival during mouse embryogenesis (Fig. 1).

Role of SAPK/JNK in apoptosis regulation

It has been proposed that SAPK/JNK activation triggers the mitochondria-dependent apoptosis in response to many types of stress, including UV-irradiation. Both *Jnk1*$^{-/-}$ *Jnk2*$^{-/-}$ and *sek1*$^{-/-}$ *mkk7*$^{-/-}$ mouse embryonic fibroblasts (MEFs) exhibited profound defects in stress-induced apoptosis (*15, 16*). These results strongly suggest that the SAPK/JNK activation directly regulates mitochondria-dependent apoptosis in the pro-apoptotic direction. In contrast, *sek1*$^{-/-}$ *mkk7*$^{-/-}$ ES cells show normal apoptotic responses, including DNA fragmentation and

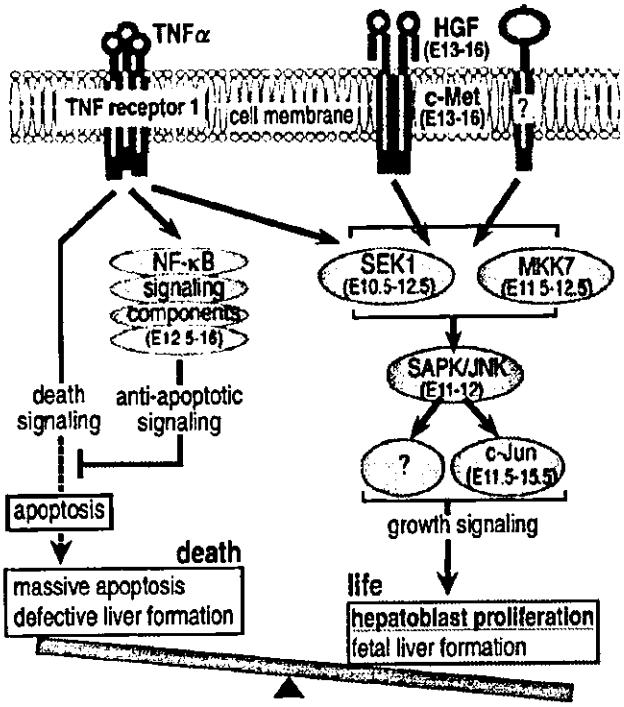

Fig. 1. **A proposed model for SAPK/JNK signaling pathway in hepatoblasts.** The numbers in parentheses are dates of embryonic lethality reported in previous papers. TNFα elicits a wide range of biological responses, such as inflammation, tumor necrosis, differentiation, cell proliferation, and apoptosis, through the stimulation of its receptor, TNFR1. The induction of apoptosis, NF-κB activation, and SAPK/JNK activation are simultaneously mediated through TNFR1. SAPK/JNK activation is involved in cell proliferation, while activation of NF-κB protects against the apoptosis in hepatoblasts (*13*).

caspase 3 activation, even though *apaf1*$^{-/-}$ ES cells exhibit profound defects in the mitochondria-dependent apoptosis (*17*). In those *sek1*$^{-/-}$ *mkk7*$^{-/-}$ ES cells, the SAPK/JNK activation by various stresses was completely abolished. Normal apoptotic responses without SAPK/JNK activation were also observed in fibroblasts derived from *sek1*$^{-/-}$ *mkk7*$^{-/-}$ ES cells. These results raised the question of whether SAPK/JNK activation is indeed required for the induction of cell death in response to apoptosis inducers. Thus, the physiological role of SAPK/JNK activation in cell survival and apoptosis is controversial, being suggested to have a pro-apoptotic, an anti-apoptotic, or no function (*18*).

From our recent results, it appears that the various roles of SAPK/JNK activation in apoptosis depend on the cell types and conditions observed. While late passage *mkk7*$^{-/-}$ MEFs are resistant to cell death in the same manner as *Jnk1*$^{-/-}$ *Jnk2*$^{-/-}$ and *sek1*$^{-/-}$ *mkk7*$^{-/-}$ MEFs (*15, 16*), *mkk7*$^{-/-}$ MEFs at earlier cell passages (passages 1–4) undergo apoptosis in response to UV exposure with the same kinetics and to the same extent as wild-type MEFs (*14*). These results support the notion that SAPK/JNK activation is not always involved in apoptosis, but this activation rather regulates apoptosis in a signal-specific (and perhaps cell type-dependent) manner. Our results in MEFs indicate that the 'history' and passage number of cells is a critical determinant of cell death susceptibility in the absence of MKK7 expression.

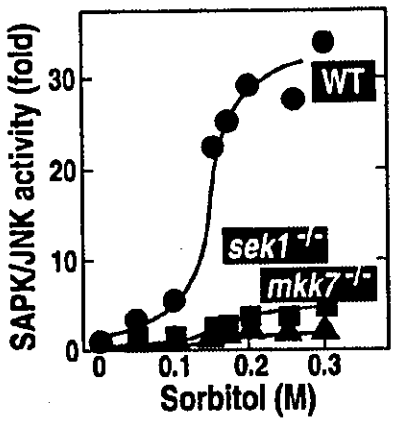

Fig. 2. **SAPK/JNK activation in response to hyper-osmolar stress (sorbitol) requires both SEK1 and MKK7 in ES cells.** Wild-type, *sek1*$^{-/-}$, and *mkk7*$^{-/-}$ ES cells were stimulated with the indicated concentrations of sorbitol for 30 min.

SAPK/JNK activation as a molecular switch in an all-or-none manner

Recently, Ferrell *et al.* have proposed the interesting concept that SAPK/JNK-signaling cascade could, in principle, function as a sensitivity amplifier, which converts graded inputs into more switch-like outputs, allowing the cascade to filter out noise and yet still respond decisively to supra-threshold stimuli (*19, 20*). They have shown in *Xenopus* oocytes, HeLa cells, HEK293 cells, and Jurkat T cells that SAPK/JNK responds to physiological and pathological stimuli, such as progesterone and sorbitol, in an all-or-none manner. The activation of SAPK/JNK by the stimuli was graded at the level of a population of oocytes; however, at the level of an individual oocyte, the stimulatory response appeared to be switch-like. Indeed, we have also observed a very steep concentration-dependent response in the activation of SAPK/JNK by hyper-osmolar stress, sorbitol, in wild-type murine embryonic stem (ES) cells but not in *sek1*$^{-/-}$ and *mkk7*$^{-/-}$ cells (Fig. 2) (*21*). This suggests that the all-or-none type MAPK activation also occurs in mammalian cells at an individual cell level only when the two MAPKKs are simultaneously activated. Therefore, this MAPK signaling should strictly proceed without errors basically through two separate signals, one that activates SEK1 and one that activates MKK7. The full activation of SAPK/JNK by SEK1 and MKK7 may be required for hepatoblast proliferation (Fig. 1).

Molecular mechanism of SAPK/JNK activation in living cells

Activation of SAPK/JNK requires the dual phosphorylation of Tyr and Thr residues located in a Thr-Pro-Tyr motif in the activation loop between VII and VIII of the kinase domain. The phosphorylation is catalyzed by the dual specificity kinases, SEK1 and MKK7, which are capable of catalyzing the phosphorylation of both Thr and Tyr residues. Recent studies have shown that SEK1 preferentially phosphorylates the Tyr residue, and MKK7 the

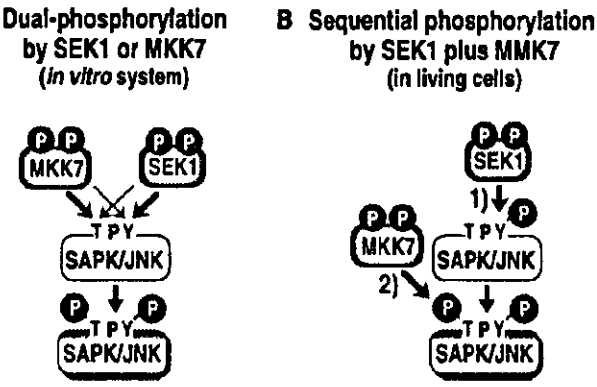

Fig. 3. **Schematic description of SAPK/JNK phosphorylation by SEK1 and MKK7 *in vitro* and *in vivo*.** A: Synergistic activation of SAPK/JNK by the dual-specificity kinase, SEK1 or MKK7, which has been reported in *in vitro* conditions (*22–24*). B: Synergistic activation of SAPK/JNK through sequential phosphorylation by SEK1 and MKK7 in murine living cells (*21, 25*). TPY, Thr-Pro-Tyr motif.

Thr residue of SAPK/JNK *in vitro* (Fig. 3A) (*22–24*). Strong support for this activation mechanism has been obtained from studies of SEK1- and MKK7-gene disruption in ES cells (*21, 25*). The severe impairment of SAPK/JNK activation observed in *mkk7*$^{-/-}$ ES cells was accompanied by a loss of the Thr-phosphorylation of SAPK/JNK, without marked reduction in its Tyr-phosphorylation level. On the other hand, Thr-phosphorylation of SAPK/JNK in *sek1*$^{-/-}$ ES cells was also attenuated, in addition to a decreased level of its Tyr-phosphorylation. These results indicate that the Tyr and Thr residues of SAPK/JNK are sequentially phosphorylated by SEK1 and MKK7, respectively, in stress-stimulated living cells (Fig. 3B).

Conclusion

SAPK/JNK activation by SEK1 and MKK7 is required for embryonic hepatoblast proliferation. The full activation of SAPK/JNK occurs only when the two MAPKKs are simultaneously activated. The Tyr and Thr residues of SAPK/JNK are sequentially phosphorylated by SEK1 and MKK7, respectively, in living cells.

SAPK/JNK may either protect or enhance sensitivity to apoptosis depending on the cell type, stimuli, and the latency of the activation of the MAPK. Our recent results in MEFs indicate that the "history" and passage number of cells are a critical determinant of cell death susceptibility in the absence of MKK7 expression. In this apoptotic pathway, SAPK/JNK seems to function through its effects on gene expression but not a direct effect on the effectors of apoptosis. These new findings could also solve the controversial data that have been obtained in different cell types and in different laboratories.

REFERENCES

1. Davis, R.J. (2000) Signal transduction by the JNK group of MAP kinases. *Cell* **103**, 239–252
2. Chang, L. and Karin, M. (2001) Mammalian MAP kinase signalling cascades. *Nature* **410**, 37–40
3. Weston, C.R. and Davis, R.J. (2002) The JNK signal transduction pathway. *Curr. Opini. Genes Dev.* **12**, 14–21
4. Manning, A.M. and Davis, R.J. (2003) Targeting JNK for therapeutic benefit: from junk to gold? *Nat. Rev. Mol. Drug Disc.* **2**, 554–565
5. Nishina, H., Nakagawa, K., Azuma, N., and Katada, T. (2003) Activation mechanism and physiological roles of stress-activated protein kinase/c-Jun NH_2-terminal kinase in mammalian cells. *J. Biol. Regul. Homeost. Agents.* **17**, 295–302
6. Wada, T. and Penninger, J.M. (2004) Mitogen-activated protein kinases in apoptosis regulation. *Oncogene* **23**, 2838–2849
7. Kuan, C.Y., Yang, D.D., Roy, D.R., Davis, R.J., Rakic, P., and Flavell, R.A. (1999) The Jnk1 and Jnk2 protein kinases are required for regional specific apoptosis during early brain development. *Neuron* **22**, 667–676
8. Sabapathy, K., Jochum, W., Hochedlinger, K., Chang, L., Karin, M., and Wagner, E.F. (1999) Defective neural tube morphogenesis and altered apoptosis in the absence of both JNK1 and JNK2. *Mech. Dev.* **89**, 115–124
9. Nishina, H., Fischer, K.D., Radvanyi, L., Shahinian, A., Hakem, R., Rubie, E.A., Bernstein, A., Mak, T.W., Woodgett, J.R., and Penninger, J.M. (1997) Stress-signalling kinase Sek1 protects thymocytes from apoptosis mediated by CD95 and CD3. *Nature* **385**, 350–353
10. Yang, D., Tournier, C., Wysk, M., Lu, H.T., Xu, J., Davis, R.J., and Flavell, R.A. (1997) Targeted disruption of the MKK4 gene causes embryonic death, inhibition of c-Jun NH2-terminal kinase activation, and defects in AP-1 transcriptional activity. *Proc. Natl Acad. Sci. USA* **94**, 3004–3009
11. Ganiatsas, S., Kwee, L., Fujiwara, Y., Perkins, A., Ikeda, T., Labow, M.A., and Zon, L.I. (1998) SEK1 deficiency reveals mitogen-activated protein kinase cascade crossregulation and leads to abnormal hepatogenesis. *Proc. Natl Acad. Sci. USA* **95**, 6881–6886.
12. Nishina, H., Vaz, C., Billia, P., Nghiem, M., Sasaki, T., Pompa, J.L., Furlonger, K., Paige, C., Hui, C.-C., Fischer, K.D., Kishimoto, H., Iwatsubo, T., Katada, T., Woodgett, J.R., and Penninger, J.M. (1999) Defective liver formation and liver cell apoptosis in mice lacking the stress signaling kinase SEK1/MKK4. *Development* **126**, 505–516
13. Watanabe, T. Nakagawa, K, Ohata, S, Kitagawa, D., Nishitai, G., Seo, J., Tanemura, S., Shimizu, N., Kishimoto, H., Wada, T., Aoki, J., Arai, H., Iwatsubo, T., Mochita, M., Watanabe, T., Satake, M., Ito, Y., Matsuyama, T., Mak, T.W., Penninger, J.M., Nishina, H., and Katada, T. (2002) SEK1/MKK4-mediated SAPK/JNK signaling participates in embryonic hepatoblast proliferation via a pathway different from NF-κB-induced antiapoptosis. *Dev Biol.* **250**, 332–347
14. Wada, T., Joza, N., Cheng, H.-Y.M., Sasaki, T., Kozieradzki, I., Bachmaier, K., Katada, T., Schreiber, M., Wagner, E.F., Nishina, H., and Penninger, J.M. (2004) MKK7 couples stress signaling to G2/M cell cycle progression and cellular senescence. *Nat. Cell Biol.* **6**, 215–226
15. Tournier, C., Hess, P., Yang, D.D., Xu, J., Turner, T.K., Nimnual, A., Bar-Sagi, D., Jones, S.N., Flavell, R.A., and Davis, R.J. (2000) Requirement of JNK for stress-induced activation of the cytochrome c–mediated death pathway. *Science* **288**, 870–874
16. Tournier, C., Dong, C., Turner, T.K., Jones, S.N., Flavell, R.A., and Davis, R.J. (2001) MKK7 is an essential component of the JNK signal transduction pathway activated by proinflammatory cytokines. *Genes Dev.* **15**, 1419–1426
17. Nishitai, G., Shimizu, N., Negishi, T., Kishimoto, H., Nakagawa, K., Kitagawa, D., Watanabe, T., Momose, H., Ohata, S., Tanemura, S., Asaka, S., Kubota, J., Saito, R., Yoshida, H., Mak, T.W., Wada, T., Penninger, J.M., Azuma, N., Nishina, H., and Katada, T. (2003) Stress induces mitochondria-mediated apoptosis independent of SAPK/JNK activation in ES cells. *J. Biol. Chem.* **279**, 1621–1626
18. Lin, A. (2002) Activation of the JNK signaling pathway: breaking the brake on apoptosis. *Bioessays* **25**, 17–24

19. Bagowski, C.P. and Ferrell, J.E. (2001) Bistability in the JNK cascade. *Curr. Biol.* **11**, 1176–1182
20. Bagowski, C.P., Besser, J., Frey, C.R., Ferrell, J.E. (2003) The JNK cascade as a biochemical switch in mammalian cells: Ultrasensitive and all-or-none responses. *Curr. Biol.* **13**, 315–320
21. Kishimoto, H., Nakagawa, K., Watanabe, T., Kitagawa, D., Momose, H., Seo, J., Nishitai, G., Shimizu, N., Ohata, S., Tanemura, S., Asaka, S., Goto, T., Fukushi, H., Yoshida, H., Suzuki, A., Sasaki, T., Wada, T., Penninger, J.M., Nishina, H., and Katada, T. (2003) Different Properties of SEK1 and MKK7 in Dual Phosphorylation of Stress-induced Activated Protein Kinase SAPK/JNK in Embryonic *Stem Cells. J. Biol. Chem.* **278**, 16595–16601
22. Lawler, S., Fleming, Y., Goedert, M., and Cohen, P. (1998) Synergistic activation of SAPK1/JNK1 by two MAP kinase kinases *in vitro. Curr. Biol.* **8**, 1387–1390
23. Lisnock, J., Griffin, P., Calaycay, J., Franz, B., Parsons, J., O'Keefe, S.J., and LoGrasso, P. (2000) Activation of JNK3α1 requires both MKK4 and MKK7: Kinetic characterization of *in vitro* phosphorylated JNK3α1. *Biochemistry* **39**, 3141–3148
24. Fleming, Y., Armstrong, C.G., Morrice, N., Paterson, A., Goedert, M., and Cohen, P. (2000) Synergistic activation of stress-activated protein kinase 1/c-Jun N-terminal kinase (SAPK1/JNK) isoforms by mitogen-activated protein kinase 4 (MKK4) and MKK7. *Biochem. J.* **352**, 145–154
25. Wada, T., Nakagawa, K., Watanabe, T., Nishitai, G., Seo, J., Kishimoto, H., Kitagawa, D., Sasaki, T., Penninger, J.M., Nishina, H., and Katada, T. (2001). Impaired synergistic activation of stress activated protein kinase SAPK/JNK in mouse embryonic stem cells lacking SEK1/MKK4. *J. Biol. Chem.* **276**, 30892–30897